Polymer Bulletin (2024) 81:6325–6348
https://doi.org/10.1007/s00289-023-05013-y

ORIGINAL PAPER

Polypyrrole confined in network of composite hydrogel as adsorbent for enhanced adsorption of Cr(VI) in aqueous solutions

Xuejiao Zhang[1] · Wenjie Zou[1] · Li Ding[1] · Jun Chen[1]

Received: 24 April 2023 / Revised: 17 July 2023 / Accepted: 20 September 2023 /
Published online: 29 September 2023

Abstract

The treatment of Cr(VI) wastewater containing hexavalent chromium is a difficult problem. The World Health Organization (WHO) "Drinking Water Quality Standard" stipulates that the maximum allowable limit of chromium in drinking water is 0.05 mg/L. It is very necessary to develop an adsorbent for efficiently removing Cr(VI) in water. In this paper, a composite porous hydrogel adsorbent of sepiolite/humic acid/polyvinyl alcohol@polypyrrole (SC/HA/PVA@PPy) was prepared by Pickering emulsion template-in-situ oxidative polymerization, and the enhancement effect of this design idea on the adsorption performance of PPy was studied with heavy metal ion hexavalent chromium Cr(VI) as the target adsorbate. The morphology and structure of the composite adsorbent were characterized by FESEM, EDX and FT-IR, which confirmed the successful compounding of PPy with SC/HA/PVA and effectively avoided the agglomeration of PPy. The adsorption performance of Cr(VI) was systematically studied through the experiments of solution pH, adsorption dosage, adsorption isotherm and adsorption kinetics. The adsorption capacity of SC/HA/PVA@PPy for Cr(VI) can reach 970.31 mg/g-PPy, which is about 44 times higher than that of pure PPy (21.87 mg/g), indicating that the experimental design can effectively avoid PPy agglomeration and exert its potential adsorption performance. The fitting results of adsorption isotherm are more in line with Langmuir model ($R^2 = 0.912$, 0.975, 0.991 at three temperatures), and the thermodynamic parameters reveal that the adsorption process is a spontaneous endothermic process. The adsorption kinetics proved that the adsorption process of Cr(VI) mainly followed the pseudo-second-order kinetic model ($R^2 = 0.957$). The regeneration study shows that the adsorbent can be recycled. In addition, according to the FESEM-EDX, FTIR and XPS analysis of the adsorbent before and after adsorption, the removal of Cr(VI) was mainly enhanced by ion exchange, electrostatic attraction and chemical reduction. The peak of Cr element in EDX spectrum after adsorption provide direct evidence for the adsorption of Cr(VI). SC/HA/PVA@PPy adsorbent

Extended author information available on the last page of the article

has good adsorption performance and strong stability, which has great development prospects in wastewater treatment.

Keywords Porous hydrogel · Polypyrrole · Hexavalent chromium · Adsorption · Wastewater treatment

Introduction

As we all know, heavy metal ions in water not only have a bad influence on the environment, but also are very harmful to human health [1–4]. Especially hexavalent chromium Cr(VI), which is highly toxic. Heavy metal Cr(VI) is ubiquitous in various industrial wastewater, and a large amount of wastewater containing Cr(VI) will be produced during electroplating and surface treatment. In addition, the wastewater from leather, tanning, textile, pigments and dyes, paint, wood processing, petroleum refining industry and photographic film production also contains a lot of Cr(VI) [5, 6]. It will cause serious damage to human nervous system, liver, blood and bones, because Cr(VI) can diffuse through the cell membrane in the form of CrO_4^{2-} or $HCrO_4^-$ ions after entering the human body, and accumulate in the body and is difficult to be metabolized [7–9]. The World Health Organization (WHO) "Drinking Water Quality Standard" stipulates that The maximum allowable limit of chromium in drinking water is 0.05 mg/L. Therefore, it is urgent to treat Cr(VI) polluted wastewater. There are numerous technologies for treating Cr(VI), such as chemical precipitation [10], membrane filtration [11], adsorption, and biological treatment [12]. Among many technologies for treating hexavalent chromium, adsorption method has attracted much attention because of its advantages of simplicity, high efficiency, low cost and no secondary pollution [13–15]. The adsorption technology mainly depends on the performance of adsorbent, which determines the adsorption efficiency and cost.

Polypyrrole (PPy) has attracted much attention in wastewater treatment due to its advantages of low cost, non-toxicity, stable environment, easy synthesis and good possibility of chemical modification [16, 17]. The redox mechanism involved in the doping and undoping process in PPy is beneficial to the adsorption of Cr(VI) in wastewater. In addition, there are some positively charged nitrogen atoms in PPy chain, which will adsorb anions in aqueous solution through ion exchange and electrostatic action and keep the charge neutral. Therefore, it has good adsorption capacity for Cr(VI) [18–20]. However, polypyrrole particles will reunite with each other due to π-π stacking, which limits the exchange between doped anions (such as Cl^-) and Cr(VI) anions. On the other hand, the adsorption performance will also be affected by the reduction of the contact area between polypyrrole and Cr(VI) [21, 22]. Polypyrrole powder can't exert high adsorption capacity because of its lack of porous structure and low surface area [23]. Solving the problem of polypyrrole is easy agglomeration and giving full play to its adsorption advantages are the research hotspots of efficient polypyrrole-based adsorption materials.

Composite method is one of the most effective methods to improve the easy agglomeration characteristics of polypyrrole [24]. The physical and chemical properties of single materials are always inferior to those of composite materials. The composite adsorbent after introducing matrix materials into polypyrrole can not only improve the dispersibility of polypyrrole, but also cooperate with the advantages of the two materials to effectively enhance the adsorption performance [6, 25]. Polyvinyl alcohol (PVA)-based hydrogels can be crosslinked to form a hydrophilic three-dimensional network structure, which has attracted much attention in the field of adsorption because of its non-toxicity, low cost, simple process, good chemical and mechanical stability and fast adsorption rate [26, 27]. As a matrix material, PVA-based hydrogel can provide a uniform dispersion system for polypyrrole and enhance the adsorption performance and mechanical strength.

Composite hydrogels with porous structure can provide adsorbents with faster adsorption rate and stronger adsorption capacity [28, 29]. Pickering emulsion template method is an excellent template for preparing various porous hydrogels, which has strong anti-coalescence, good long-term stability and biocompatibility. Pickering emulsion is stabilized by solid particles, and the irreversible adsorption of solid particles makes it very stable [30, 31]. In addition, the droplet size of Pickering emulsion can be adjusted by the solid particles, thus determining the pore size of the adsorbent [32]. Clay, as a solid particle with colloidal size, large reserves and low cost, is the preferred material for stabilizing Pickering emulsion. Sepiolite (SC) is a typical natural clay material with fibrous morphology, wide sources and high specific surface area. The surface is negatively charged (because Si^{4+} is replaced by other cations), and it has a certain adsorption capacity, which has great advantages in stabilizing Pickering emulsion [33, 34].

In order to reduce the agglomeration of PPy and increase the exposure of active adsorption sites, so that the potential adsorption performance of PPy can be brought into play, a composite porous hydrogel adsorbent of sepiolite/humic acid/polyvinyl alcohol@polypyrrole (SC/HA/PVA@PPy) was prepared by Pickering emulsion template in-situ oxidative polymerization. Compounding PPy with SC/HA/PVA can not only effectively prevent PPy from agglomeration, but also improve the adsorption capacity of hydrogel for Cr(VI). Specifically, a stable SC/HA/PVA oil-in-water Pickering emulsion was prepared with SC/HA composite colloidal particles as stabilizer. There is negatively charged SC at the droplet interface, which combines with PPy through electrostatic interaction (PPy contains positively charged nitrogen-containing groups), thus limiting PPy to the emulsion droplet interface for in-situ oxidative polymerization. Then PVA was crosslinked by freeze–thaw cycle method [35] to form a three-dimensional network structure to obtain hydrogel. Hydrogel network also plays a limiting role in PPy. Finally, SC/HA/PVA@PPy composite porous adsorbent was obtained by solvent volatilization- freeze drying (Fig. 1). The adsorbents were characterized by FESEM, EDX, FT-IR and XPS. Cr(VI) was taken as the target to determine the actual adsorption performance of PPy in the prepared hydrogel. The effects of solution pH, adsorbent dosage, adsorption time, initial concentration and temperature of Cr(VI) on the adsorption performance were investigated, and the main mechanism of Cr(VI) adsorption was analyzed. The SC/HA/PVA@PPy composite porous hydrogel prepared in this study to adsorb Cr(VI), which

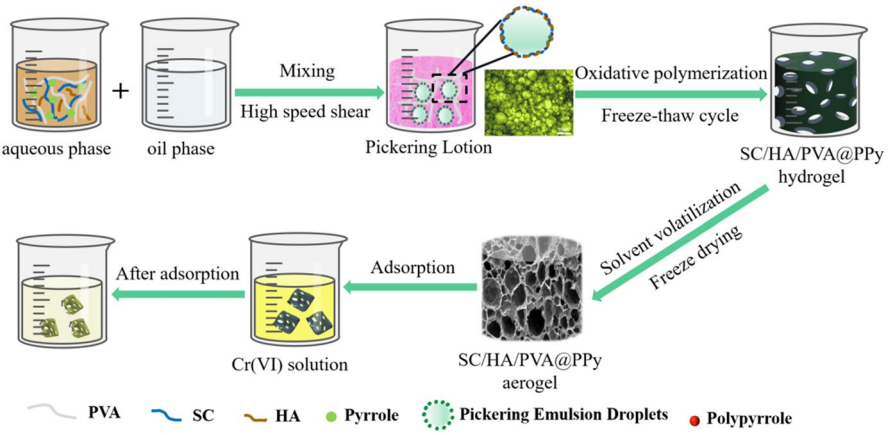

Fig. 1 Schematic diagram of preparation of SC/HA/PVA@PPy adsorbent and adsorption of Cr(VI)

gives full play to the adsorption potential of PPy itself, improves the utilization rate of PPy, and is also in line with the concept of developing environmental-friendly adsorbents. Another is to utilize composite colloidal particles with abundant and low-cost sepiolite and humic acid to synergistically stabilize Pickering emulsion, which enriches the stabilization methods of Pickering emulsion.

Methods

Raw materials

Sepiolite (SC) was purchased by TOLSA, S.A (Spain). Humic acid (HA) was purchased from houma Jiayou Humic Acid Co., Ltd. Polyvinyl alcohol (PVA, polymerization degree is about 1700), cyclohexane (C_6H_{12}), potassium dichromate ($K_2Cr_2O_7$), pyrrole (C_4H_5N), acetone (C_3H_6O), 1,5-diphenylcarbazide, phosphoric acid (H_3PO_4), sulfuric acid (H_2SO_4), ammonium persulfate (APS) ($(NH_4)_2S_2O_8$), hydrochloric acid (HCl), sodium hydroxide (NaOH) and ethanol (C_2H_6O) are purchased from Sinopharm Chemical Reagents Co., Ltd.(Shanghai, China). All stock solutions were prepared with deionized water for material preparation and adsorption experiments.

Synthesis of SC/HA/PVA@PPy adsorbent

The pH value of 11 g deionized water was adjusted to 11, and 0.064 g SC and 0.0064 g HA were uniformly dispersed in it to obtain a uniform SC/NaHA solution. Add 3.2 mL hydrochloric acid solution (5 M) to obtain SC/HA composite colloidal particle solution. Then, 16 g of 10% PVA solution and 0.16 g of pyrrole were added in turn. After stirring evenly to obtain water phase, 61.70 mL of cyclohexane (oil phase) was added, and then a uniform and stable oil-in-water Pickering emulsion

was obtained through high-speed shearing. 0.56 g ammonium persulfate was dissolved in 4 mL hydrochloric acid solution (0.5 M), then added into Pickering emulsion as oxidant, slowly stirred until the color was uniform, and stood for 12 h. After polymerization, the hydrogel was obtained by freeze–thaw cycle for 5 times. The oil phase, unreacted monomers and oligomers were removed by washing with deionized water and ethanol. Finally, SC/HA/PVA@PPy composite porous adsorbent was obtained by freeze drying.

Characterization

Optical microscope (Motic, MOTIC CHINA GROUP CO., LTD) was used to observe the droplet stability of Pickering emulsion and take photos to record the droplet size.The elemental composition and micro-morphology of the materials before and after adsorption were measured by field emission scanning electron microscope (FESEM) equipped with energy dispersion analysis system of X-ray spectrometer (EDX) (NOVA Nano SEM 430, FEI Corporation).Fourier transform infrared spectrometer (FT-IR, PerkinElmer, USA) was used to analyze the functional groups of PPy, SC/HA/PVA and SC/HA /PVA@PPy before and after adsorption. The infrared spectra were recorded in the wave number range of 400–4000 cm^{-1} at room temperature, with a spectral resolution of 4 cm^{-1} and 16 scanning times. The zeta potential at different pH values was measured by a Zetasizer Nano ZS90 instrument (Malvern, UK) at room temperature. X-ray photoelectron spectroscopy (XPS) of the materials before and after adsorption were analyzed by ESCALAB 250XI Xray photoelectron spectrometer (Thermo Fisher) with Al Kα radiation (1486.6 eV). Ultraviolet–visible spectrophotometer (UV3600, shimadzu corporation) was used to evaluate the adsorption capacity of SC/HA/PVA@PPy for Cr(VI) in the wavelength range of 500–700 nm.

Adsorption experiments

Batch experiments were carried out on SC/HA/PVA@PPy in a water bath constant temperature oscillator. The diluted $K_2Cr_2O_7$ stock solution (1000 mg/L) was used to prepare Cr(VI) solutions with different concentrations, and the pH of the solution was adjusted by adding 0.2 mol/L HCl or 0.2 mol/L NaOH. The effects of solution pH (2, 4, 6, 8, 10), adsorbent dosage (0.5–5 g/L), adsorption time (10–600 mins), initial concentration (50–250 mg/L) and temperature (298, 308, 318 K) of Cr(VI) on adsorption performance were systematically investigated. Three parallel experiments were carried out in all experiments to improve the accuracy of the experiments. The adsorption capacity was evaluated by Langmuir and Freundlich isothermal models. Thermodynamic parameters are used to analyze the thermodynamic properties of adsorption process. The adsorption mechanism and diffusion mechanism were further studied by using pseudo-first-order rate equation, pseudo-second-order rate equation and intraparticle diffusion model. According to 1,5-diphenylcarbazide spectrophotometry [36], the residual Cr(VI) ion concentration was measured by UV–vis spectrophotometer (UV3600, Shimadzu Corporation) at the wavelength

of 540 nm. The removal rate R (%) of adsorbents on Cr(VI) and the adsorbed Cr(VI) amount on per gram of adsorbent Q_t (mg/g) in time t were calculated using Eqs. (1) and (2) as follows [37]:

$$R(\%) = \frac{C_0 - C_t}{C_0} \times 100 \tag{1}$$

$$Q_t = \frac{C_0 - C_t}{m} \times V \tag{2}$$

where C_0 (mg/L) and C_t (mg/L) correspond to the initial concentrations of Cr(VI) ions and the residual concentration of Cr(VI) at time t, respectively. m(g) represents the mass of adsorbent, and V(L) represents the volume of Cr(VI) solution.

Results and discussion

Characterization of SC/HA/PVA@PPy adsorbent

The structure, pore size and micro-morphology of Pickering emulsion droplets, SC/HA/PVA and SC/HA/PVA@PPy composite adsorbents were characterized. It is observed from Fig. 2a–c that the pore diameters of SC/HA/PVA and SC/HA/PVA@PPy composite adsorbents is basically the same as the droplet size of Pickering emulsion. The results show that Pickering emulsion prepared with SC/HA composite solid particles as stabilizer has good stability, and porous hydrogel prepared with this emulsion as template also has excellent stability. The abundant circular pores in SC/HA/PVA@PPy adsorbent are highly connected. These pores can be used as water channels to accelerate the combination of adsorbate and adsorption sites, thus improving the adsorption rate. Figure 2d shows that the surface of SC/HA/PVA is smooth, while the surface of SC/HA/PVA@PPy (Fig. 2e) is rough, and PPy is evenly distributed on SC/HA/PVA@PPy, which indicates that PPy is successfully compounded on the composite adsorbent and effectively improves the agglomeration of PPy. In addition, the rough surface can provide more adsorption sites for Cr(VI) ions, thus improving the adsorption capacity. The EDX elemental analysis [38] results of SC/HA/PVA and composite adsorbent SC/ HA/PVA@PPy are shown in Fig. 2f, g. It is found that C, N, O, Si and Mg are the main elements of SC/HA/PVA. In contrast, Cl element was added to SC/HA/PVA@PPy. Obviously, the Cl element comes from the Cl^- doped with PPy. EDX confirmed the successful compounding of PPy and SC/HA/PVA.

Figure 3 shows the infrared spectra of PPy, SC/HA/PVA and SC/HA/PVA@PPy. In order to better analyze the functional groups of materials, Fig. 4 shows the FTIR spectra of SC/HA/PVA and SC/HA/ PVA@PPy separately. In curve of PPy of Fig. 3, the bands at 1558, 1480, 1046 and 925 cm^{-1} are determined by the C=C stretching vibration peak, C–N stretching vibration peak, C–C in-plane and out-of-plane bending vibration peaks, respectively. All of these peaks belong to the characteristic peak of polypyrrole [39, 40]. It can be observed from Fig. 4 that the spectral similarity

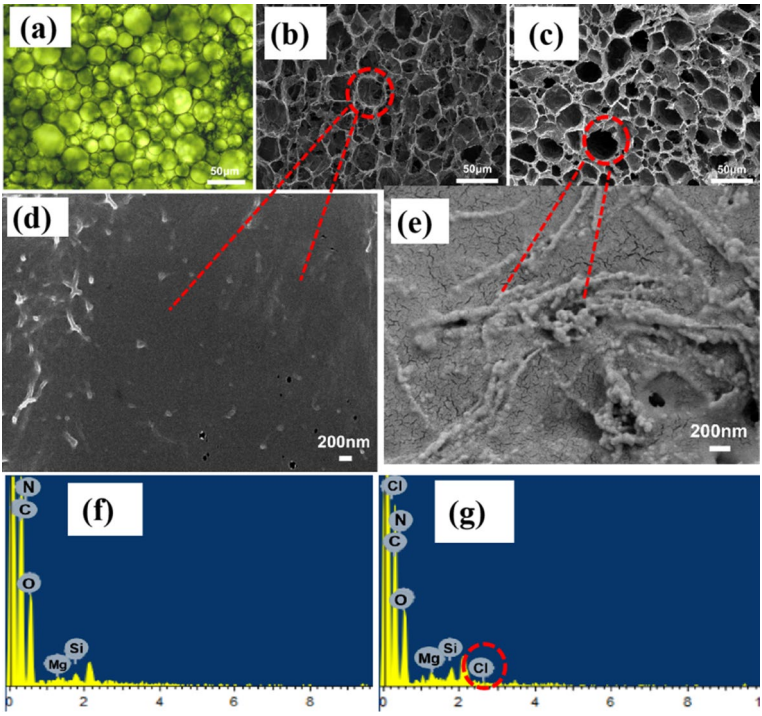

Fig. 2 Optical microscope images of Pickering emulsion droplets (**a**), Low magnification FESEM images of SC/HA/PVA and SC/HA/PVA@PPy (**b**, **c**), High magnification FESEM images of SC/HA/ PVA and SC/HA/PVA@PPy (**d**, **e**) and EDX analysis images of SC/HA/PVA (**f**), SC/HA/PVA@PPy (**g**)

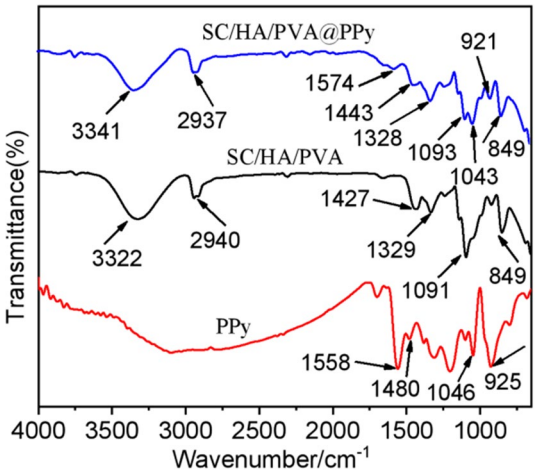

Fig. 3 FTIR diagram of PPy, SC/HA/PVA, SC/HA/PVA@PPy

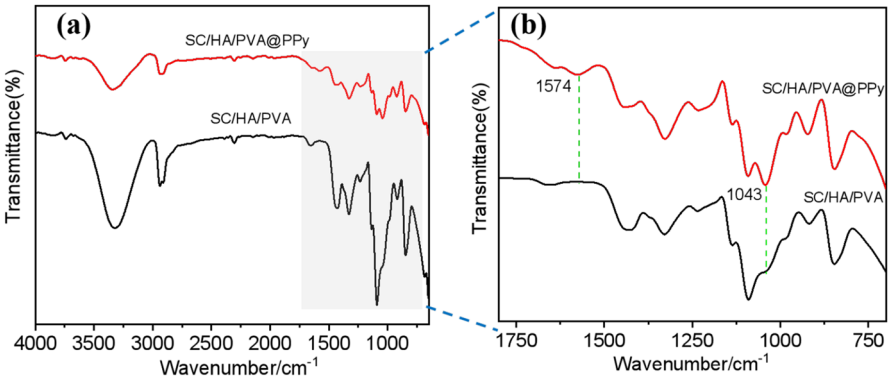

Fig. 4 FTIR comparison diagram of SC/HA/PVA and SC/HA/PVA@PPy (**a**), FTIR comparison of local amplification of SC/HA/PVA and SC/HA/PVA@PPy (**b**)

between the two is very high, which shows that the combination of PPy does not destroy the overall structure of hydrogel. SC/HA/PVA and SC/HA/PVA@PPy have a strong broad peak at 3400–3250 cm^{-1}, which is mainly due to the stretching vibration of –OH [41–43]. Among them, the N–H stretching vibration of PPy in SC/HA /PVA@PPy overlaps with –OH. The peak near 2940 cm^{-1} comes from the asymmetric and symmetric stretching vibration of C–H [44], while the peaks at 1092 and 849 cm^{-1} correspond to the tensile vibration of Si–O and the deformation vibration of Mg–OH [45], respectively. In SC/HA/PVA@PPy, the spectral peaks at 1574 and 1043 cm^{-1} are attributed to the C=C tensile vibration and the C–C in -plane bending vibration of PPy [46], respectively, which are the characteristic peaks of PPy. The above results showed that PPy and SC/HA/PVA were successfully compounded.

The surface charge of adsorbent directly affects the adsorption performance of materials. The Zeta potential of the adsorbent at different pH values was measured and shown in Fig. 5. The zero charge value (pHzpc) of SC/HA/PVA@PPy was

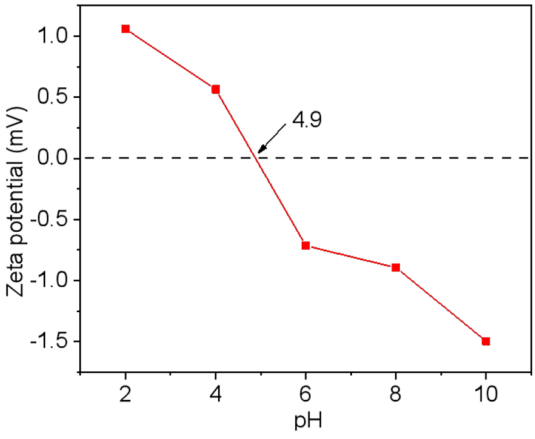

Fig. 5 Zeta potentials of SC/HA/PVA@PPy at different pH values (C_0 = 100 mg/L, t = 12 h, T = 298 K, adsorbent dosage = 1 g/L)

determined to be 4.9. When the pH of the solution is less than 4.9, the surface of SC/HA/PVA@PPy is positively charged [47], and the removal amount of Cr(VI) oxygen anion increases due to the enhancement of electrostatic interaction. On the contrary, when the pH of the solution is greater than 4.9, the surface of SC/HA/PVA@PPy is negatively charged [48], which enhances the electrostatic repulsion and reduces the removal amount of Cr(VI) oxygen anion.

Sorption properties of SC/HA/PVA@PPy

Comparison of adsorption capacity before and after material compounding

The adsorption capacity of Cr(VI) was calculated to determine the actual adsorption performance of PPy on the prepared composite adsorbent. Table 1 displays that the maximum adsorption capacity of SC/HA/PVA@PPy for Cr(VI) can reach 125.37 mg/g, which is obviously higher than that of pure PPy (21.87 mg/g) [49] in the literature and SC/HA/PVA (44.45 mg/g). Furthermore, according to the percentage of PPy and SC/HAPVA in SC/HA/PVA@PPy, it can be calculated that the actual adsorption capacity of Cr(VI) by PPy is 970.31 mg/g-PPy, which is also greatly improved compared with the pure PPy in the literature. The results show that the combination of PPy and SC/HA/PVA can not only significantly improve the adsorption capacity of adsorbent. It can also effectively prevent the reunion of PPy, which gives full play to the potential ability and enhancement in adsorbing Cr(VI).

Effect of pH

The pH value of the solution will directly affect the surface charge of the adsorbent and the existing form of metal ions, so the pH value of the solution is one of the important parameters affecting the adsorption performance of the adsorbent during the adsorption process. The adsorption capacity of SC/HA/PVA@PPy for Cr(VI) was studied in the range of pH 2–10, and the result is shown in Fig. 6a. The adsorption capacity reached the optimal value at pH 2, and then decreased rapidly with the increase of pH. Figure 6b is a distribution diagram of that exist forms of Cr(VI) at different pH value. It can be seen that in the pH range of 2–6, Cr(VI) mainly exists in the form of $Cr_2O_7^{2-}$ or $HCrO_4^-$ anion, when the pH > 6, the main existing form of Cr(VI) changes to CrO_4^{2-} [50]. This corresponds to the adsorption result in Fig. 6a. Under acidic conditions, $Cr_2O_7^{2-}$ and $HCrO_4^-$ ions can replace the doped Cl^- and adsorb Cr(VI) anions through ion exchange. On the other hand,

Table 1 Comparison of adsorption capacity of different samples

Sample	Py content (%)	q_e (mg/g)	Unit PPy adsorption capacity (mg/g)	References
SC/HA/PVA	0	44.45	0	Present study
Pure PPy	100	21.87	21.87	[49]
SC/HA/PVA@PPy	8.74	125.37	970.31	Present study

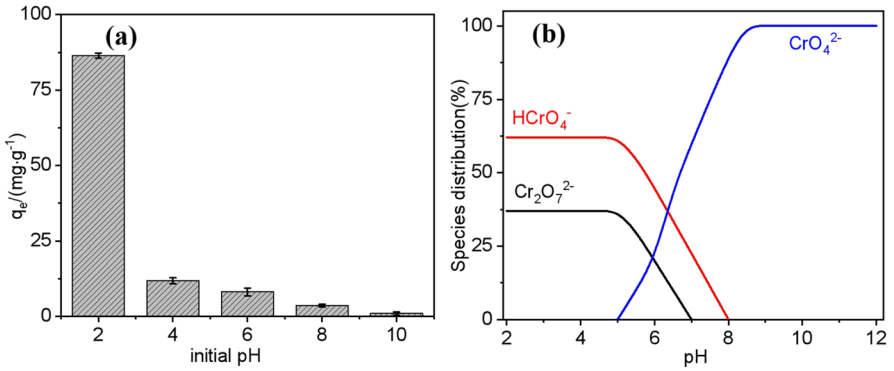

Fig. 6 Effect of solution pH on adsorption performance (**a**) and species distribution of Cr(VI) at different pH (**b**) (C_0 = 100 mg/L, t = 12 h, T = 298 K, adsorbent dosage = 1 g/L)

the protonated amino groups on the surface of SC/HA/PVA@PPy are positively charged and adsorb Cr(VI) anions through electrostatic interaction. In addition, the adsorbent has a high redox potential at this time, which can promote the reduction of Cr(VI) to Cr(III) [51]. However, in the aqueous solution with pH > 6, the adsorbent is de-doped, and excessive OH^- in the solution will compete with CrO_4^{2-} for adsorption sites. Meanwhile, the deprotonation of amino group reduces the positive charge on the adsorbent surface, which hinders the interaction with Cr(VI). Therefore, that adsorption performance of the adsorbent decrease. The above analysis is consistent with the discussion of zeta potential.

Effect of adsorbent dose

Investigating the influence of adsorbent dosage is helpful to weigh the cost and actual adsorption benefit. In this experiment, the effect of dosage on the adsorption

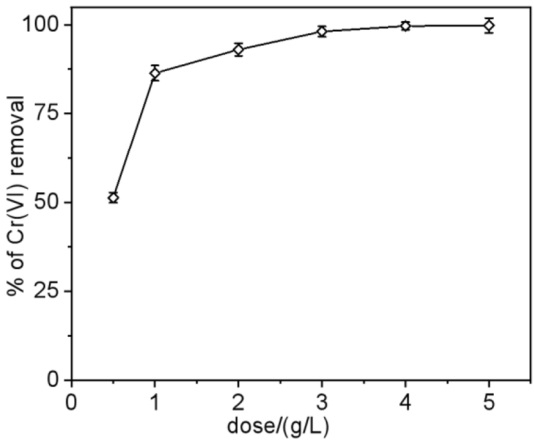

Fig. 7 Effect of adsorbent dosage on adsorption performance (C_0 = 100 mg/L, t = 12 h, T = 298 K, pH 2)

of Cr(VI) by SC/HA/PVA@PPy composite was studied in the range of 0.5–5 g/L. As shown in Fig. 7, with the increase of dosage from 0.5 to 5 g/L, the removal rate of Cr(VI) increased from 51.35 to 99.81%. The relationship between the removal rate of Cr(VI) and the dosage of adsorbent did not increase linearly, but increased rapidly to slowly. In the process of 0.5–1 g/L, the concentration of adsorbate is much higher than that of adsorbent, and there are a large number of available adsorption sites [52], the adsorption rate increases rapidly. With the increasing amount of adsorbent, the ratio of Cr(VI) anion to available active sites decreases, and the driving force to overcome the resistance of solid–liquid mass transfer also decreases [53], so the increase of adsorption rate becomes slow.

Adsorption kinetics

Adsorption equilibrium time is also an important factor to investigate the performance of adsorbents. Figure 8 shows the change of Cr(VI) adsorbed by SC/HA/PVA@PPy with time. Clearly, the adsorption rate is very fast in the first 10 mins, and about 77% of the adsorption is directly completed. With the increase of reaction time, the adsorption rate gradually increases until it reaches equilibrium at 480 min. At the initial stage of adsorption, there are a large number of available adsorption sites on the adsorbent, and the concentration of Cr(VI) in the local micro-environment of adsorbent-adsorbate is high. At the later stage of adsorption, most adsorption sites were occupied and the effective adsorption sites decreased. With the decrease of Cr(VI) concentration in the local micro-environment of adsorbent -adsorbate, the later adsorption rate gradually slows down until the adsorption equilibrium is reached.

Adsorption kinetics can provide useful information for understanding the adsorption process of Cr(VI) on adsorbents. The pseudo-first-order kinetic model [54, 55], pseudo-second-order kinetic model [56] and intraparticle diffusion model [57] were introduced to fit the adsorption data to understand the kinetic mechanism of adsorbent. The nonlinear equations of the three models are as follows:

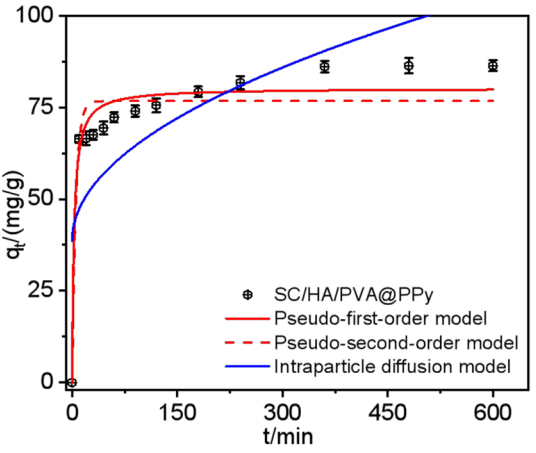

Fig. 8 Kinetics of SC/HA/PVA@PPy adsorption of Cr(VI) (C_0 = 100 mg/L, T = 298 K, adsorbent dosage = 1 g/L = 0.01 g, pH 2)

Pseudo-first-order:

$$q_t = q_e\left(1 - e^{-k_1 t}\right) \tag{3}$$

Pseudo-second-order:

$$q_t = \frac{k_2 q_e^2 t}{1 + k_2 q_e t} \tag{4}$$

Intraparticle diffusion model:

$$q_t = k_3 t^{0.5} + C \tag{5}$$

where q_t (mg/g) is the amount of Cr(VI) adsorbed at time t, q_e (mg/g) is equilibrium adsorption amount, k_1 (1/min) is the pseudo-first-order rate constant, k_2 (g/(mg min)) is the pseudo-second-order rate constant, k_3 (mg/(g $min^{0.5}$)) is the intraparticle diffusion constant, whereas C is the boundary layer thickness constant.

Figure 8 and Table 2 show the fitting results of kinetic experiments. Compared with the pseudo- first-order model, the pseudo-second-order model has a higher correlation coefficient ($R^2 = 0.976$), and its calculated adsorption capacity q_e (80.24 mg/g) is also closer to the experimental value q_e (86.41 mg/g). It can be concluded that the adsorption process of Cr(VI) by SC/HA/PVA@PPy composite follows the pseudo-second-order kinetic model, which holds that the main mechanism of Cr(VI) adsorption is chemical adsorption [58, 59]. The intraparticle diffusion model was used to further study the adsorption rate control steps and diffusion mechanism. According to the intraparticle diffusion diagram (Fig. 8) and the fitting parameters (Table 2), the correlation coefficient ($R^2 = 0.508$) is not good, the fitting curve does not pass through the coordinate origin, and the value of the boundary layer thickness constant C is not 0, which indicates that intraparticle diffusion is not

Table 2 Adsorption kinetic models and parameters for removal of Cr(VI) on SC/HA/PVA@PPy

Parameters	
C_0 (mg/L)	100
q_e(exp) (mg/g)	86.41
Pseudo-first-order	
k_1 (1/min)	0.438
q_e (mg/g)	76.76
R^2	0.957
Pseudo-second-order	
k_2 (g/(mg·min))	0.004
q_e (mg/g)	80.24
R^2	0.976
Intraparticle diffusion	
k_3 (mg/(g·$min^{0.5}$))	2.726
C	38.693
R^2	0.508

the only rate control factor in the adsorption process of Cr(VI), and may be affected by the membrane diffusion [60].

Adsorption isotherm

The adsorption isotherm can determine the maximum adsorption capacity of adsorbent. In this experiment, the adsorption capacity of adsorbent in different Cr(VI) concentrations was tested at three temperatures (298, 308 and 318 K). Langmuir (single-layer homogeneous adsorption) [61] and Freundlich (multi-layer heterogeneous adsorption) isotherm models [62] were used to fit the adsorption data. The nonlinear fitting equation of the model is as follows:

Langmuir:

$$q_e = \frac{K_L q_m C_e}{1 + K_L C_e} \tag{6}$$

Freundlich:

$$q_e = K_F C_e^{1/n} \tag{7}$$

where C_e (mg/L) is the Cr(VI) mass concentration in solution equilibrium, q_e (mg/g) is equilibrium adsorption amount, q_m (mg/g) is the maximum adsorption capacity, K_L (L/mg) is the Langmuir constant related to adsorption energy, which represents the affinity of the adsorbent for the adsorbent. K_F (mg/g) and n are the Freundlich isotherm constants related to adsorption capacity and intensity, respectively. It can be seen from Fig. 9a that the adsorption capacity of SC/HA/PVA@PPy increases with the increase of the initial concentration of Cr(VI) in the solution, and then tends to balance gradually. This is because there are many empty adsorption sites on the adsorbent at first. Once Cr(VI) comes into contact with the adsorbent, it will quickly occupy the adsorption sites, so the adsorption capacity will increase rapidly. With

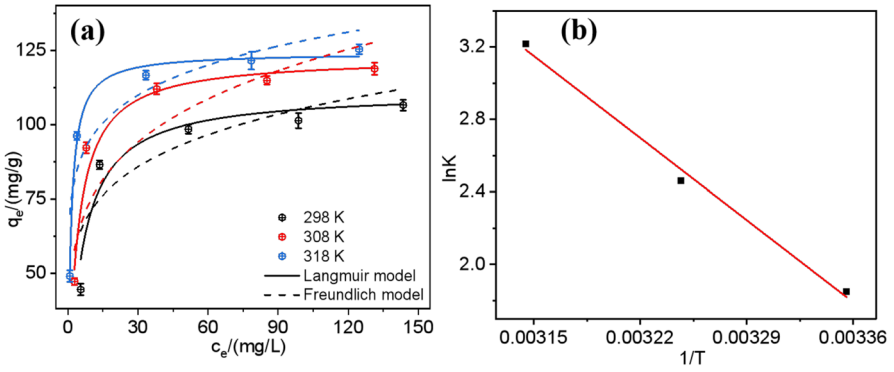

Fig. 9 Isotherm of SC/HA/PVA@PPy adsorption of Cr(VI) at different temperatures (**a**), Plot of lnK- 1/T to determine the thermodynamic parameters of Cr(VI) adsorption onto SC/HA/PVA@PPy (**b**) (t = 12 h, adsorbent dosage = 1 g/L = 0.01 g, pH 2)

the continuous increase of Cr(VI) concentration, the adsorption sites have gradually reached saturation and the adsorption capacity will steadily become balanced. With the increase of temperature, the adsorption capacity also increases, reaching the optimal adsorption capacity of 125.37 mg/g at 318 K, which indicates that the temperature has a positive correlation with the adsorption performance of the material, and the adsorption process of the material is an endothermic reaction process.

The fitting results of adsorption isotherm model are shown in Fig. 9a and Table 3. Obviously, the data fitted by Langmuir model is better and R^2 is higher, which reflects that Langmuir model is more suitable to describe the adsorption process of Cr(VI) by SC/HA/PVA@PPy than Freundlich model. The results suggest that the main mechanism of Cr(VI) adsorption on the composite is monolayer adsorption, and the active sites are evenly distributed on the adsorbent [63, 64]. In addition, with the temperature rising from 298 to 318 K, the maximum adsorption capacity q_m calculated by Langmuir model increased from 111 to 124.13 mg/g, indicating that temperature rise is beneficial to adsorption.

Comparing the adsorption of Cr(VI) by SC/HA/PVA@PPy with other porous hydrogel adsorbents (Table 4). It is found that compared with porous hydrogel adsorbents in these literatures, SC/HA/PVA @PPy has higher adsorption capacity for removing Cr(VI), and the optimal adsorption capacity can reach 125.37 mg/g at 318 K, which is higher than that in most literatures. Moreover, as can be confirmed by the analysis results in Table 1 above, the actual adsorption capacity of PPy for Cr(VI) can reach 970.31 mg/g-PPy according to the percentages of PPy and SC/HA/PVA in SC/HA@PPy, which gives full play to the adsorption potential of PPy itself, improves the utilization rate of PPy, and conforms to the concept of developing environmentally friendly adsorbents. The results show that SC/HA/PVA@PPy has great research value in removing Cr(VI).

Thermodynamics studies

In order to study the thermodynamic properties of adsorption process (endothermic or exothermic, randomness and spontaneity), we calculated the following thermodynamic parameters. Thermodynamic parameters such as standard Gibbs free energy change (ΔG°), enthalpy change (ΔH°) and entropy change (ΔS°) for the adsorption of Cr(VI) by SC/HA/PVA@PPy (initial concentration of 100 mg/L) have been determined by the following equation [69]:

Table 3 Adsorption isotherm models and parameters for removal of Cr(VI) on SC/HA/PVA@PPy

T/K	Langmuir constants			Freundlich constants		
	q_m (mg/g)	K_L (L/mg)	R^2	K_F (mg/g)	1/n	R^2
298	111.00	0.176	0.912	48.05	0.170	0.732
308	122.66	0.252	0.975	46.54	0.207	0.855
318	124.13	0.811	0.991	71.15	0.128	0.809

Table 4 Comparison of adsorption of SC/HA/PVA@PPy for Cr(VI) with porous hydrogel adsorbents

Adsorbent	q_m (mg/g)	pH	Initial Cr(VI) concentration range (mg/L)	References
Polyaniline/poly(vinyl alcohol) aerogels	41.2	2.0	13–50	[27]
Fe_3O_4 nanoparticles functionalized polyvinyl Alcohol/chitosan magnetic composite hydrogel	55	3.0	0–100	[65]
Chitosan-based hydrogel	73.14	4.5	50–500	[66]
Chitosan/montmorillonite composite hydrogels	78	5.5–6.0	50–200	[67]
Chitosan/reduced graphene oxide/ montmorillonite composite hydrogels	87.03	2.0	0–240	[68]
SC/HA/PVA@PPy	125.37	2.0	50–250	Present study

$$\ln K = \frac{\Delta S^0}{R} - \frac{\Delta H^0}{RT} \tag{8}$$

$$\Delta G^0 = -RT \ln K \tag{9}$$

$$K = \frac{C_0 - C_e}{C_e} \tag{10}$$

where K (L/g) is thermodynamic equilibrium constant, R is the ideal gas constant (8.314 J/mol/K), T is temperature (K), C_0 (mg/L) is the initial concentrations of Cr(VI) ions and C_e (mg/L) is the Cr(VI) mass concentration in solution equilibrium. The thermodynamic parameters obtained are shown in Fig. 9b and Table 5. The positive value of ΔH° proves that the adsorption process is endothermic, and high temperature can promote the adsorption of Cr(VI), which is consistent with the experimental results of temperature. Moreover, the value of ΔH° < 80 kJ/mol, which indicates that the adsorption of Cr(VI) by SC/HA/PVA@PPy is a physisorption process [70, 71]. This is not in contradiction with the kinetic results, indicating that the adsorption of Cr(VI) on the adsorbent can be carried out by physics, chemistry or the combination of the two. The positive value of ΔS° indicates that the randomness of solid–liquid interface increases during adsorption [72]. At all experimental temperatures, ΔG° is negative, indicating that the adsorption process of Cr(VI) is spontaneous, and the greater the negative value of ΔG°, the better the adsorption [73]. The values of ΔG° in Table 5 is negatively correlated with temperature, which further confirms that high temperature is beneficial to adsorption.

Analysis of regenerative performance

Evaluating the regeneration efficiency of adsorbent materials for further use is very important for studying a cost-effective adsorbent material to remove Cr(VI) in industrial wastewater. In this experiment, $NaHCO_3$ (0.5 M) solution was used as eluent, washed with distilled water, and HCl (2M) solution was used as dopant to reactivate the adsorption site, so the adsorption cycle was repeated for four times. The Fig. 10 shows the removal efficiency of SC/HA/PVA@PPy in each adsorption cycle. After four cycles, the removal efficiency of Cr(VI) by SC/HA/PVA@PPy decreased from 86.4% to 50.1%. Cr(VI) is not completely desorbed from the adsorbent or reduced to Cr(III), which may be the reasons for the low reuse rate. The results show that SC/

Table 5 Thermodynamic parameters of adsorption of Cr(VI) by SC/HA/PVA@PPy

T(K)	Thermodynamic parameters		
	ΔG° (kJ/mol)	ΔH° (kJ/mol)	ΔS° (kJ/mol/K)
298	−15.75	53.811	0.196
308	−29.98		
318	−66.03		

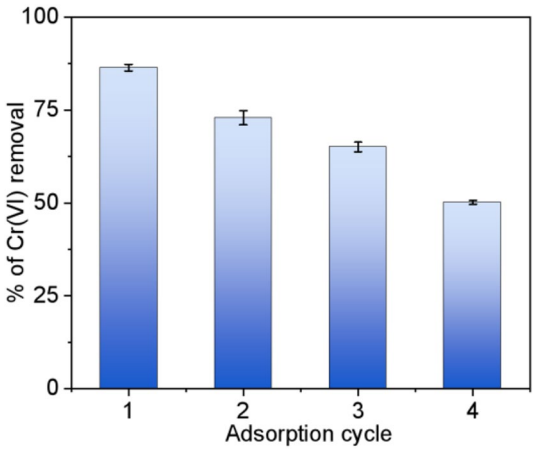

Fig. 10 Regeneration cycle of SC/HA/PVA@PPy adsorption of Cr(VI) (C_0 = 100 mg/L, T = 298 K, adsorbent dosage = 1 g/L = 0.01 g, pH 2, t = 12 h)

HA/PVA@PPy composite porous hydrogel has good regeneration and reusability, and it is an effective adsorbent for treating Cr(VI) ion polluted wastewater.

Adsorption mechanism of Cr(VI) by SC/HA/PVA@PPy

The surface morphology and elemental composition of SC/HA/PVA@PPy before and after adsorption of Cr(VI) were evaluated by FESEM-EDX. Comparing Figs. 2c and 11a, there is almost no difference in the structure of the adsorbent before and after adsorption, and the porous structure remains stable, which proves that the composite adsorbent has stable structure and high mechanical strength. As can be seen from Figs. 2e and 11b, many sepiolite fibers are staggered on the rough adsorbent surface, while a large number of PPy are evenly distributed on the adsorbent surface and sepiolite fibers, which indicates that PPy is very stably fixed on SC/HA/PVA@PPy. Figure 11c is the EDX element spectrum after Cr(VI) adsorption. Compared with before adsorption (Fig. 2g), there is an obvious Cr element peak in the energy spectrum after adsorption, while the Cl element peak disappears, indicating that Cr(VI) anion is adsorbed by replacing the doped Cl^-. Other authors who have studied the adsorption of Cr(VI) by PPy-based adsorbent [74, 75] have also reported a similar trend. EDX spectrum is the direct evidence that Cr(VI) is adsorbed on SC/HA/PVA@PPy by ion exchange.

The FTIR spectra of SC/HA/PVA@PPy composite adsorbent before and after adsorption were compared, and the possible mechanism of Cr(VI) adsorption was analyzed according to the changes of spectral peaks. It can be observed from Fig. 11d that after absorbing Cr(VI), the whole spectral peak shifts to low wavenumber. It is speculated that Cr(VI) anion replaced the doped Cl^-, which affected the conjugated structure of PPy chain, and the delocalization degree of charge along the polymer chain was limited, which led to the red shift of the peak [22]. After adsorption, the tensile vibration peak of C–N moved from 1443 to 1414 cm^{-1}, which was the characteristic peak of PPy, and its weakening indicated that amino functional groups participated in the adsorption reaction [76]. In addition, the broad

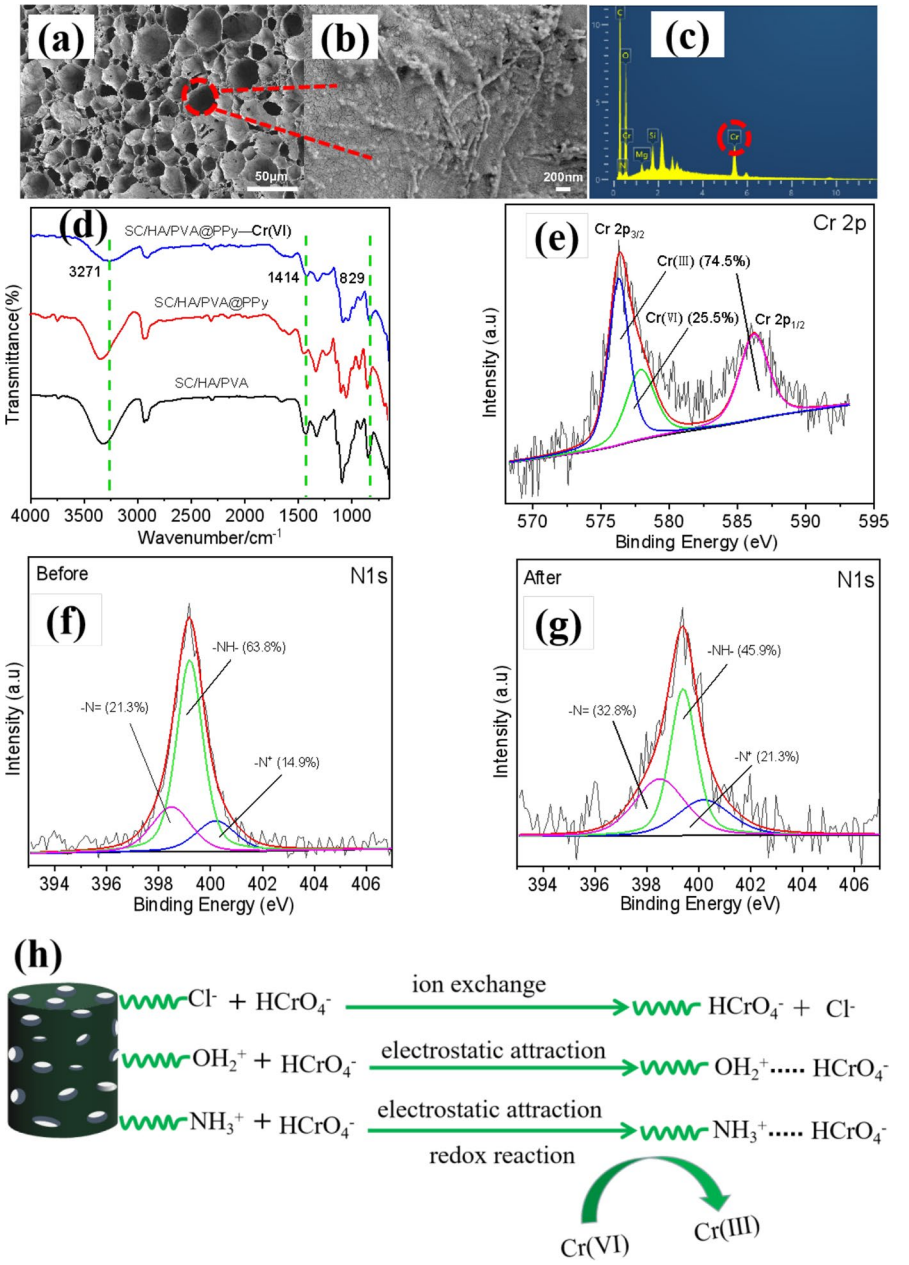

Fig. 11 Low and high magnification FESEM (**a**, **b**), EDX (**c**), FTIR spectra (**d**) and high-resolution XPS spectra of Cr 2p (**e**) of SC/HA/PVA@PPy after Cr(VI) adsorption, high-resolution XPS spectra of N 1s (**f**, **g**) of SC/HA/PVA@PPy before and after Cr(VI) adsorption, scheme of the adsorption mechanism of Cr(VI) (**h**)

peak at 3341 cm^{-1} is red-shifted to 3271 cm^{-1}, and the intensity is obviously weakened, which indicates that hydroxyl and amino groups play a role in Cr(VI) adsorption [77]. The peak of 849 cm^{-1} moves to 829 cm^{-1} and the peak width becomes slightly larger, which may be because the Cr–O bond formed overlaps with Mg–OH [78]. After the adsorption reaction, only some peak shifts and intensities changed, while the whole peak shape remained basically unchanged, which indicated that the adsorption reaction would not destroy the structure of the adsorbent.

To investigate the adsorption mechanism of Cr(VI) on SC/HA/PVA@PPy in detail, XPS analysis was carried out. Figure 11e shows the high-resolution XPS spectrum of Cr 2p of SC/HA/PVA@PPy after Cr(VI) adsorption. The spectrum of Cr 2p can be divided into three peaks: 577.9 (Cr $2p_{3/2}$), 576.3 (Cr $2p_{3/2}$) and 586.2 (Cr $2p_{1/2}$) eV. The first peak corresponds to Cr(VI), and the last two peaks correspond to Cr(III). According to the calculation of peak area, there are about 74.5% Cr(III) and 25.5% Cr(VI) on the adsorbent, which proved that redox reaction occurred on the adsorbent, and part of the adsorbed Cr(VI) was reduced to Cr(III) [79]. The reduction reaction needs to get electrons, and the amino group in PPy can be used as an electron donor group to provide electrons for Cr(VI) reduction [80]. Therefore, the N 1s before and after Cr(VI) adsorption was characterized by high-resolution XPS spectrum (Fig. 11f and Fig. 11g). The XPS spectrum of N 1s before adsorption can be deconvolved into three different peaks at 398.5, 399.2 and 400.2 eV, which are attributed to 21.3% imine nitrogen (–N=), 63.8% amine nitrogen (–NH–) and 14.9% charged nitrogen ($–N^+$) groups, respectively [81]. Among them, the existence of ($–N^+$) is due to the protonation reaction of some imines under acidic conditions. After adsorption, the percentage of nitrogen component changed. The proportion of –NH– decreased to 45.9%, while the proportion of –N= increased to 32.8%, which proved that part of –NH– on the adsorbent participated in the reduction reaction of Cr(VI) as an electron donor group [82]. In addition, the increase of the proportion of $–N^+$ corresponds to the decrease of pH value in the solution after adsorption. The charged nitrogen ($–N^+$) groups can generate electrostatic attraction with Cr(VI) to adsorb Cr(VI). XPS analysis results show that the adsorption mechanism of Cr(VI) may include electrostatic attraction and redox reaction.

Hence, the adsorption mechanism scheme of Cr(VI) is given in Fig. 11h. The results of FESEM- EDX, FTIR and XPS analysis show that the adsorption mechanism of Cr(VI) by SC/HA/PVA@PPy involves ion exchange, electrostatic attraction and redox reaction.

Conclusion

A new type of Cr(VI) adsorbent was synthesized based on the double "defining effect" of hydrogel network and Pickering emulsion template on PPy, which effectively enhanced the adsorption capacity of PPy for Cr(VI) in water. The initial pH of solution, adsorption dose, reaction time, initial concentration of Cr(VI) and temperature will all affect the performance of adsorbent. Adsorption kinetics and thermodynamic experiments show that the adsorption of Cr(VI) by SC/HA/PVA@PPy is a spontaneous endothermic single-layer adsorption reaction, and the adsorption

process of Cr(VI) on the adsorbent is complex, which can be carried out by physical, chemical or combination of the two. The possible mechanisms of adsorption of Cr(VI) by SC/HA/PVA@PPy are ion exchange, electrostatic attraction and redox reaction. The fast adsorption rate of the adsorbent (77% within 10 mins), easy separation from water and high utilization rate of PPy (970.31 mg/g-PPy) make the SC/HA/PVA@PPy composite adsorbent have a certain application prospect in the field of wastewater treatment.

Acknowledgements This work was supported by Preparation of lignite humic acid-based magnetic composite microspheres and their adsorption properties for heavy metal ions, National Natural Science Foundation of China (21576001).

Author contributions All authors contributed to the study conception and design. XZ Process the data and write the manuscript. WZ, LD Work together to complete material preparation, data collection and analysis. JC Directed, revised, and supplemented the manuscript. All authors commented on previous versions of the manuscript, and all authors read and approved the final manuscript.

Data availability The dataset produced and processed during this research is available upon reasonable request from the corresponding author.

Declarations

Conflict of interest The authors have declared the absence of conflict of interest.

References

1. Li LB, Zhao LR, Ma J, Tian YH (2020) Preparation of graphene oxide/chitosan complex and its adsorption properties for heavy metal ions. Green Process Synth 9(1):294–303
2. Lin ZK, Yang YR, Liang ZZ, Zeng LZ, Zhang AP (2021) Preparation of chitosan/calcium alginate/bentonite composite hydrogel and its heavy metal ions adsorption properties. Polymers 13(11):1891–1909
3. Ahmad K, Shah H-U-R, Ashfaq M, Nawaz H (2022) Removal of decidedly lethal metal arsenic from water using metal organic frameworks: a critical review. Rev Inorg Chem 42(2):197–227
4. Parveen S, Naseem AH, Ahmad K, Shah HUR, Aziz T, Ashfaq M, Rauf D (2022) Design, synthesis and spectroscopic characterizations of medicinal hydrazide derivatives and metal complexes of malonic ester. Curr Bioact Compd 19(4):e221221199270
5. Yang JB, Huang B, Lin MZ (2020) Adsorption of hexavalent chromium from aqueous solution by a chitosan/bentonite composite: isotherm, kinetics, and thermodynamics studies. J Chem Eng Data 65(5):2751–2763
6. Mdlalose L, Balogun M, Setshedi K, Chimuka L, Chetty A (2020) Performance evaluation of polypyrrole–montmorillonite clay composite as a re-usable adsorbent for Cr(VI) remediation. Polym Bull 78(8):4685–4697
7. Taşdelen B, Çifçi Dİ, Meriç S (2021) Preparation and characterization of chitosan/AMPS/ kaolinite composite hydrogels for adsorption of methylene blue. Polym Bull 79(11):9643–9662
8. Orooji Y, Nezafat Z, Nasrollahzadeh M, Kamali TA (2021) Polysaccharide-based (nano)materials for Cr(VI) removal. Int J Biol Macromol 188:950–973
9. Shan HM, Zeng CY, Zhao CR, Zhan HB (2021) Iron oxides decorated graphene oxide/chitosan composite beads for enhanced Cr(VI) removal from aqueous solution. Int J Biol Macromol 172:197–209
10. Ayub A, Srithilat K, Fatima I, Panduro-Tenazoa NM, Ahmed I, Akhtar MU, Shabbir W, Ahmad K, Muhammad A (2022) Arsenic in drinking water: overview of removal strategies and role of chitosan biosorbent for its remediation. Environ Sci Pollut Res Int 29(43):64312–64344

11. Ahmad K, H-u-R S, Khan MS, Iqbal A, Potrich E, Amaral LS, Rasheed S, Nawaz H, Ayub A, Naseem K, Muhammad A, Yaqoob MR, Ashfaq M (2022) Lead In drinking water: adsorption method and role of zeolitic imidazolate frameworks for its remediation: a review. J Clean Prod 368:133010
12. Fallatah AM, Shah HUR, Ahmad K, Ashfaq M, Rauf A, Muneer M, Ibrahim MM, El-Bahy ZM, Shahzad A, Babras A (2022) Rational synthesis and characterization of highly water stable MOF@GO composite for efficient removal of mercury ($Hg^{(2+)}$) from water. Heliyon 8(10):e10936
13. Matome SM, Makhado E, Katata-Seru LM, Maponya TC, Modibane KD, Hato MJ, Bahadur I (2020) Green synthesis of polypyrrole/nanoscale zero valent iron nanocomposite and use as an adsorbent for hexavalent chromium from aqueous solution. S Afr J Chem Eng 34:1–10
14. Pakade VE, Tavengwa NT, Madikizela LM (2019) Recent advances in hexavalent chromium removal from aqueous solutions by adsorptive methods. RSC Adv 9(45):26142–26164
15. Ahmad K, Nazir MA, Qureshi AK, Hussain E, Najam T, Javed MS, Shah SSA, Tufail MK, Hussain S, Khan NA, H-u-R S, Ashfaq M (2020) Engineering of Zirconium based metal-organic frameworks (Zr-MOFs) as efficient adsorbents. Mater Sci Eng B 262:114766
16. Ji YJ, Xu FY, Zhang PL, Xu YY, Zhang GL (2021) Green synthesis of poly(pyrrole methane)-based adsorbent for efficient removal of chromium(VI) from aqueous solution. J Clean Prod 293:126197
17. Alghamdi AA, Al-Odayni AB, Saeed WS, Al-Kahtani A, Alharthi FA, Aouak T (2019) Efficient Adsorption of Lead (II) from Aqueous Phase Solutions Using Polypyrrole-Based Activated Carbon. Materials 12(12): 2020
18. Karthikeyan P, Elanchezhiyan SS, Meenakshi S, Park CM (2021) Magnesium ferrite-reinforced polypyrrole hybrids as an effective adsorbent for the removal of toxic ions from aqueous solutions: Preparation, characterization, and adsorption experiments. J Hazard Mater 408:124892
19. Zhang WJ, Wang YX, Fei YL, Wang YL, Zhang ZX, Kou M, Feng QC, Wang S, Du XY, Rossi M (2021) One-pot synthesis of magnetic polypyrrole nanotubes for adsorption of Cr(VI) in aqueous solution. Adv Mater Sci Eng 2021:1–15
20. Fang W, Jiang XY, Luo HJ, Geng JJ (2018) Synthesis of graphene/SiO2@polypyrrole nanocomposites and their application for Cr(VI) removal in aqueous solution. Chemosphere 197:594–602
21. Zhou TT, Liang QW, Zhou X, Luo HJ, Chen W (2021) Enhanced removal of toxic hexavalent chromium from aqueous solution by magnetic Zr-MOF@polypyrrole: performance and mechanism. Environ Sci Pollut Res 28(11):13084–13096
22. Xiang L, Niu CG, Tang N, Lv XX, Guo H, Li ZW, Liu HY, Lin LS, Yang YY, Liang C (2021) Polypyrrole coated molybdenum disulfide composites as adsorbent for enhanced removal of Cr(VI) in aqueous solutions by adsorption combined with reduction. Chem Eng J 408(15):127281
23. Ye X, Xu QC, Xu J (2019) Oxidant-templating fabrication of pure polypyrrole hydrogel beads as a highly efficient dye adsorbent. RSC Adv 9(11):5895–5900
24. Anush SM, Chandan HR, Gayathri BH, Asma MN, Vishalakshi B, Kalluraya B (2020) Graphene oxide functionalized chitosan-magnetite nanocomposite for removal of Cu(II) and Cr(VI) from waste water. Int J Biol Macromol 164:4391–4402
25. Karaer Yağmur H (2020) Synthesis and characterization of conducting polypyrrole/bentonite nanocomposites and in-situ oxidative polymerization of pyrrole: adsorption of 4-nitrophenol by polypyrrole/bentonite nanocomposite. Chem Eng Commun 207(8):1171–1183
26. Radoor S, Karayil J, Jayakumar A, Nandi D, Parameswaranpillai J, Lee J, Siengchin S (2022) Polyvinyl alcohol/guar gum-based bio-adsorbent for the removal of cationic and anionic dyes from aqueous solution. Polym Bull. https://doi.org/10.1007/s00289-022-04552-0
27. Zaghlol S, Amer WA, Shaaban MH, Ayad MM, Bober P, Stejskal J (2020) Conducting macroporous polyaniline/poly(vinyl alcohol) aerogels for the removal of chromium(VI) from aqueous media. Chem Pap 74(9):3183–3193
28. Wu ZY, Zhang P, Zhang HH, Li XT, He YF, Qin PW, Yang CH (2022) Tough porous nanocomposite hydrogel for water treatment. J Hazard Mater 421:126754
29. Ren LL, Xu J, Zhang YC, Zhou J, Chen DH, Chang ZY (2019) Preparation and characterization of porous chitosan microspheres and adsorption performance for hexavalent chromium. Int J Biol Macromol 135:898–906
30. Jiang QX, Horozov T, Bismarck A (2022) One-pot approach to fabrication of porous polymers from Pickering emulsion templates. Polymer 261:125406
31. Wang XD, He JX, Ma LH, Yan B, Shi LY, Ran R (2021) Self-assembling graphene oxide/ modified amphipathic hydroxyethyl cellulose hybrid stabilized Pickering emulsion polymerization for functional hydrogel. Colloids Surf A Physicochem Eng Aspects 610:125742

32. Zhao H, Yang YQ, Chen Y, Li J, Wang L, Li CS (2022) A review of multiple Pickering emulsions: solid stabilization, preparation, particle effect, and application. Chem Eng Sci 248:117085
33. Yu H, Zhu YF, Xu J, Wang AQ (2020) Fabrication porous adsorbents templated from modified sepiolite-stabilized aqueous foams for high-efficient removal of cationic dyes. Chemosphere 259:126949
34. Chen J, Hong XQ, Xie QD, Li DK, Zhang QF (2014) Sepiolite fiber oriented-polypyrrole nanofibers for efficient chromium(VI) removal from aqueous solution. J Chem Eng Data 59(7):2275–2282
35. Omer AM, Sadik WAA, El-Demerdash AGM, Tamer TM, Khalifa RE, Mohyeldin MS, Abdelwahed NA (2020) Fabrication of semi-interpenetrated PVA/PAMPS hydrogel as a reusable adsorbent for cationic methylene blue dye: isotherms, kinetics and thermodynamics studies. Polym Bull 78(11):6649–6673
36. Huang DL, Liu CH, Zhang C, Deng R, Wang RZ, Xue WJ, Luo H, Zeng GM, Zhang Q, Guo XY (2019) Cr(VI) removal from aqueous solution using biochar modified with Mg/Al-layered double hydroxide intercalated with ethylenediaminetetraacetic acid. Bioresour Technol 276:127–132
37. Chen J, Hong XQ, Xie QD, Tian M, Li K, Zhang QF (2015) Exfoliated polypyrrole/montmorillonite nanocomposite with flake-like structure for Cr(VI) removal from aqueous solution. Res Chem Intermed 41(12):9655–9671
38. Saleem F, Abid MZ, Rafiq K, Rauf A, Ahmad K, Iqbal S, Jin R, Hussain E (2023) Synergistic effect of Cu/Ni cocatalysts on CdS for sun-light driven hydrogen generation from water splitting. Int J Hydrogen Energy. https://doi.org/10.1016/j.ijhydene.2023.05.048
39. Qi FF, Ma TY, Liu Y, Fan YM, Li JQ, Yu Y, Chu LL (2020) 3D superhydrophilic polypyrrole nanofiber mat for highly efficient adsorption of anionic azo dyes. Microchem J 159:105389
40. Kera NH, Bhaumik M, Pillay K, Ray SS, Maity A (2018) m-Phenylenediamine-modified polypyrrole as an efficient adsorbent for removal of highly toxic hexavalent chromium in water. Mater Today Commun 15:153–164
41. Aziz T, Nasim HA, Ahmad K, Shah HU, Parveen S, Ahmad MM, Majeed H, Galal AM, Rauf A, Ashfaq M (2023) Rational synthesis, biological screening of azo derivatives of chloro-phenylcarbonyl diazenyl hydroxy dipyrimidines/thioxotetrahydropyrimidines and their metal complexes. Heliyon 9(1):e12492
42. Hafsa SHUR, Ahmad K, Ashfaq M, Oku H (2023) Free radical scavenging, antibacterial potentials and spectroscopic characterizations of benzoyl thiourea derivatives and their metal complexes. J Mol Struct 1272:134162
43. Ahmad K, Shah HUR, Ahmad M, Ahmed MM, Naseem K, Riaz NN, Muhammad A, Ayub A, Ahmad M, Ahmad Z, Munwar A, Rauf A, Hussain R, Ashfaq M (2022) Comparative study between two zeolitic imidazolate frameworks as adsorbents for removal of organoarsenic, As (III) and As (V) species from water. Braz J Anal Chem 9(36):78–97
44. Ahmad K, Shah HUR, Ashfaq A, Ashfaq M, Kashif M, Naseem HA, Aziz T, Parveen S, Hafsa NI (2021) Synthesis of new series of phenyldiazene based metal complexes for designing most active antibacterial and antifungal agents. J Chem Soc Pakistan 43(5):578–586
45. Senol-Arslan D (2021) Isotherms, kinetics and thermodynamics of pb(ii) adsorption by crosslinked chitosan/sepiolite composite. Polym Bull 79(6):3911–3928
46. Xiang L, Niu CG, Tang N, Lv XX, Guo H, Li ZW, Liu HY, Lin LS, Yang YY, Liang C (2021) Polypyrrole coated molybdenum disulfide composites as adsorbent for enhanced removal of Cr(VI) in aqueous solutions by adsorption combined with reduction. Chem Eng J 408
47. Guo X, Liu A, Lu J, Niu X, Jiang M, Ma Y, Liu X, Li M (2020) Adsorption mechanism of hexavalent chromium on biochar: kinetic, thermodynamic, and characterization studies. ACS Omega 5(42):27323–27331
48. Ayub A, Irfan A, Raza ZA, Abbas M, Muhammad A, Ahmad K, Munwar A (2021) Development of poly(1-vinylimidazole)-chitosan composite sorbent under microwave irradiation for enhanced uptake of Cd(II) ions from aqueous media. Polym Bull 79(2):807–827
49. Roy K, Mondal P, Bayen SP, Chowdhury P (2012) Sonochemical synthesis of polypyrrole salt and study of its Cr(VI) sorption-desorption properties. J Macromol Sci A 49(11):931–935
50. Liang HX, Song B, Peng P, Jiao GJ, Yan X, She D (2019) Preparation of three-dimensional honeycomb carbon materials and their adsorption of Cr(VI). Chem Eng J 367:9–16
51. Xu YL, Chen JY, Chen R, Yu PL, Guo S, Wang XF (2019) Adsorption and reduction of chromium(VI) from aqueous solution using polypyrrole/calcium rectorite composite adsorbent. Water Res 160:148–157
52. Muhammad A, Shah A, Bilal S (2019) Comparative study of the adsorption of acid blue 40 on polyaniline, magnetic oxide and their composites: synthesis. Charact Appl Mater 12(18):2854

53. Vu XH, Nguyen LH, Van HT, Nguyen DV, Nguyen TH, Nguyen QT, Ha LT (2019) Adsorption of chromium(VI) onto freshwater snail shell-derived biosorbent from aqueous solutions: equilibrium, kinetics, and thermodynamics. J Chem 2019:1–11
54. Ahmad K, Shah HU, Ashfaq M, Shah SSA, Hussain E, Naseem HA, Parveen S, Ayub A (2021) Effect of metal atom in zeolitic imidazolate frameworks (ZIF-8 & 67) for removal of Pb^{2+} & Hg^{2+} from water. Food Chem Toxicol 149:112008
55. Naseem K, Ali F, Tahir MH, Afaq M, Yasir HM, Ahmed K, Am A, Habila MA (2022) Investigation of catalytic potential of sodium dodecyl sulfate stabilized silver nanoparticles for the degradation of methyl orange dye. J Mol Struct 1262:132996
56. Ahmad K, Shah H-U-R, Parveen S, Aziz T, Naseem HA, Ashfaq M, Rauf A (2021) Metal organic framework (KIUB-MOF-1) as efficient adsorbent for cationic and anionic dyes from brackish water. J Mol Struct 1242:130898
57. Maponya TC, Ramohlola KE, Kera NH, Modibane KD, Maity A, Katata-Seru LM, Hato MJ (2020) Influence of magnetic nanoparticles on modified polypyrrole/m-phenylediamine for adsorption of Cr(VI) from aqueous solution. Polymers 12(3):679–695
58. Altun T, Kar Y (2016) Removal of Cr(VI) from aqueous solution by pyrolytic charcoals. New Carbon Mater 31(5):501–509
59. Rehman Shah HU, Ahmad K, Naseem HA, Parveen S, Ashfaq M, Rauf A, Aziz T (2021) Water stable graphene oxide metal-organic frameworks composite (ZIF-67@GO) for efficient removal of malachite green from water. Food Chem Toxicol 154:112312
60. González-López ME, Laureano-Anzaldo CM, Pérez-Fonseca AA, Arellano M, Robledo-Ortíz JR (2020) Chemically modified polysaccharides for hexavalent chromium adsorption. Sep Purif Rev 50(4):333–362
61. Langmuir I (1916) The constitution and fundamental properties of solids and liquids. Part I. Solids. J Am Chem Soc 38(11):2221–2295
62. Freundlich HMF (1906) Over the adsorption in solution. J Phys Chem 57:1100–1107
63. He Y, Guo ZL, Chen MF, Wan SC, Peng N, Fu XL, Yuan DZ, Na B (2023) Efficient adsorption of methyl orange and methylene blue dyes by a novel carbazole-based hyper-crosslinked porous polymer. J Porous Mater. https://doi.org/10.1007/s10934-023-01434-2
64. Ahmad K, Shah H-U-R, Nasim HA, Ayub A, Ashfaq M, Rauf A, Shah SSA, Ahmad MM, Nawaz H, Hussain E (2022) Synthesis and characterization of water stable polymeric metallo organic composite (PMOC) for the removal of arsenic and lead from brackish water. Toxin Rev 41(2):577–587
65. Yan EY, Cao ML, Ren XQ, Jiang J, An QL, Zhang ZY, Gao JW, Yang XY, Zhang DQ (2018) Synthesis of Fe3O4 nanoparticles functionalized polyvinyl alcohol/chitosan magnetic composite hydrogel as an efficient adsorbent for chromium (VI) removal. J Phys Chem Solids 121:102–109
66. Vilela PB, Dalalibera A, Duminelli EC, Becegato VA, Paulino AT (2019) Adsorption and removal of chromium (VI) contained in aqueous solutions using a chitosan-based hydrogel. Environ Sci Pollut Res Int 26(28):28481–28489
67. Tekay E, Aydınoğlu D, Şen S (2019) Effective adsorption of Cr(VI) by high strength chitosan/montmorillonite composite hydrogels involving spirulina biomass/microalgae. J Polym Environ 27(8):1828–1842
68. Yu P, Wang HQ, Bao RY, Liu ZY, Yang W, Xie BH, Yang MB (2017) Self-assembled sponge-like chitosan/reduced graphene oxide/montmorillonite composite hydrogels without cross-linking of chitosan for effective Cr(VI) sorption. ACS Sustain Chem Eng 5(2):1557–1566
69. Rodrigues E, Almeida O, Brasil H, Moraes D, dos Reis MAL (2019) Adsorption of chromium (VI) on hydrotalcite-hydroxyapatite material doped with carbon nanotubes: equilibrium, kinetic and thermodynamic study. Appl Clay Sci 172:57–64
70. Ghebache Z, Safidine Z, Hamidouche F, Boudieb N, Benaboura A, Trari M (2022) Elaboration and characterization of new adsorbents based on conducting PANI/zeolite HY/TiO_2 nanocomposite applied for chromate adsorption. Polym Bull. https://doi.org/10.1007/s00289-022-04500-y
71. Douinat O, Bestani B, Benderdouche N, Boucherdoud A (2021) Use of Olea europaea leaves-based activated carbon for pollutant removal from liquid effluents. Desalin Water Treat 210:258–272
72. Seghier A, Boucherdoud A, Seghier S, Benderdouche N, Hadjel M, Bestani B (2022) Equilibrium and kinetics of sorption and resorption of acid and basic dyes using the pulp of carob pods. J Dispers Sci Technol. https://doi.org/10.1080/01932691.2022.2063882:1-13
73. Guo C, Wu SJ, Gao XP, Li MY, Long HM (2021) Mechanistic study of Cr(VI) removal by modified alginate/GO composite via synergistic adsorption and photocatalytic reduction. Int J Biol Macromol 189:910–920

74. Bai L, Li Z, Zhang Y, Wang T, Lu R, Zhou W, Gao H, Zhang S (2015) Synthesis of water-dispersible graphene-modified magnetic polypyrrole nanocomposite and its ability to efficiently adsorb methylene blue from aqueous solution. Chem Eng J 279:757–766
75. Choe J, Ji J, Yu J, Jang K, Yun J, Choe S, Rim Y, Jo C (2022) Adsorption of Cr(VI) in aqueous solution by polypyrrole nanotube and polypyrrole nanoparticle; Kinetics, isotherm equilibrium, and thermodynamics. Inorg Chem Commun 145:109981
76. Bhaumik M, Maity A, Srinivasu VV, Onyango MS (2011) Enhanced removal of Cr(VI) from aqueous solution using polypyrrole/Fe3O4 magnetic nanocomposite. J Hazard Mater 190(1–3):381–390
77. Sirousazar M, Khodamoradi P (2020) Freeze-thawed humic acid/polyvinyl alcohol supramolecular hydrogels. Mater Today Commun 22:100719
78. Yang G, Tang L, Cai Y, Zeng G, Guo P, Chen G, Zhou Y, Tang J, Chen J, Xiong W (2014) Effective removal of Cr(VI) through adsorption and reduction by magnetic mesoporous carbon incorporated with polyaniline. RSC Adv 4(102):58362–58371
79. Bin YL, Liang QW, Luo HJ, Chen YY, Wang T (2023) One-step synthesis of nitrogen-functionalized graphene aerogel for efficient removal of hexavalent chromium in water. Environ Sci Pollut Res 30:6746–6757
80. Cao W, Wang ZQ, Ao HT, Yuan BL (2018) Removal of Cr(VI) by corn stalk based anion exchanger: the extent and rate of Cr(VI) reduction as side reaction. Coll Surf A Physicochem Eng Aspects 539:424–432
81. Sahu S, Bishoyi N, Patel RK (2021) Cerium phosphate polypyrrole flower like nanocomposite: a recyclable adsorbent for removal of Cr(VI) by adsorption combined with in-situ chemical reduction. J Ind Eng Chem 99:55–67
82. Yang D, Chen Y, Li J, Li YF, Song W, Li XG, Yan LG (2022) Synthesis of calcium- aluminum-layered double hydroxide and a polypyrrole decorated product for efficient removal of high concentrations of aqueous hexavalent chromium. J Colloid Interface Sci 607(Pt 2):1963–1972

Authors and Affiliations

Xuejiao Zhang[1] · Wenjie Zou[1] · Li Ding[1] · Jun Chen[1]

✉ Jun Chen
junchen@ahut.edu.cn

[1] School of Chemistry and Chemical Engineering, Anhui University of Technology, Ma Xiang Road, Maanshan 243000, People's Republic of China